# *Aconitum* and *Delphinium* sp. Alkaloids as Antagonist Modulators of Voltage-Gated Na^{+} Channels: PM3 and QSAR Investigations

Malakhat A. Turabekova,[1,2]* Bakhtiyor F. Rasulev,[2] and Mikhail G. Levkovich[2]

[1] Chemistry Department, National University of Uzbekistan named after Mirzo Ulugbek, Vuzgorodok, Tashkent, 700174, Uzbekistan

[2] Institute of Chemistry of Plant Substances, Kh. Abdullaev Str., 77, Tashkent, 700170, Uzbekistan

**Abstract**

Alkaloids of *Aconitum* and *Delphinium* plant species have been applied in eastern folk medicine owing to their wide spectrum of therapeutic action including antiarrhythmic, analgesics, neurological etc. Early pharmacological studies suggested that these neurotoxins act at site 2 of voltage-gated Na^{+} channel and allosterically modulate its function. Remarkably, despite of similar molecular structure, *Aconitum* and *Delphinium* sp. alkaloids can be divided into two distinct groups: the blockers and the openers of the sodium ion channels. It was also reported that three crucial functional residues must be present in a molecule for exhibiting channel activation: hydroxyl group at C13, benzoylester group at C14 and acetyl group at C8 of the lycoctonine skeleton. Though these alkaloids have received a great deal of attention by medicinal chemists, the literature survey resulted in little evidence on them being investigated by means of molecular modelling technique. A series of 18 antagonist alkaloids (9 blockers and 9 openers) have been selected for PM3 semiempirical studies in order to trace structure-activity (structure-toxicity) relationship at electronic level. An examination of frontier orbitals obtained by PM3 hamiltonian for ground and protonated forms of the compounds revealed that HOMOs and LUMOs were mainly represented by nitrogen atom and beznyl/benzoylester orbitals respectively and with –OH and –OCOCH$_3$ contributions being less than 1%. Hence it was concluded that opening or blocking activities are not controlled by frontier orbitals and instead biological activity is attributted to allosteric interactions of the alkaloids with the receptor site, which is in a good agreement with experiments. GA-MLRA technique was also applied for the generation of QSAR models for the set of blockers and the openers individually. Molecular size defining descriptors (MW and MR) were selected as the best properties related to toxicity for the openers' set. Quantum-chemical descriptors (energy of LUMO and HOMO-LUMO energy gap) have been identified for the blockers.

**Keywords**. *Aconitum* alkaloid, *Delphinium* alkaloid, PM3, QSAR, toxicity, Na^{+} channel modulator

| Abbreviations and notations | |
| --- | --- |
| PM3, parameterization method 3 | QSAR, quantitative structure-activity relationships |
| MLRA, multiple linear regression analysis | HOMO, highest occupied molecular orbital |
| GA, genetic algorithm | LUMO, lowest unoccupied molecular orbital |
| MW, molecular weight descriptor | ED$_{50}$, effective dose |
| MR, molar refractivity descriptor | LD$_{50}$, lethal dose |

* Correspondence author; phone: (998) 71-1627897; fax: (998) 71-1206475; E-mail: malohathon@yahoo.com

# 1 INTRODUCTION

Voltage-gated sodium channels are transmembrane proteins responsible for signal transduction and amplification, and are primary molecular targets for several groups of naturally occurring neurotoxins and a number of drugs [1-4]. One of these groups is represented by lipid-soluble neurotoxins targeting type 2 receptor site on voltage-gated $Na^+$ channels. Site 2 toxins are of very diverse chemical structures and a number of studies on mechanisms of action suggest that they promote $Na^+$ channel opening by indirect allosteric interactions [5,6]. The recent investigations showed that receptor site of these neurotoxins appears to be adjacent to or overlap with that for sodium channel blockers (anticonvulsants, antidepressants, local anaesthetics, antiarrhythmics etc.)[6].

Diterpene alkaloids isolated from *Delphinium* and *Aconitum* plant species are targets of considerable interest and studies as they belong to site 2 neurotoxins [7]. Paradoxically, despite of similar molecular structures these alkaloids exhibit antagonistic alteration of sodium channel function and therefore different therapeutic action [8-13]. In particular, aconitine-type compounds are suggested to bind with high affinity to activated sodium channels and shift conformational equillibrium toward the activated state. On the contrary, other group of alkaloids isolated from the same plant species and having very similar (heteratisine and napelline) or even identical (lycoctonine) core skeletons to aconitine are reported to posses strong antinociceptive, antiarrhythmic and antiepiletiform properties due to a blockade of the voltage-dependent sodium channel. Thus, as it was demonstrated earlier, arrhythmogenic effect of aconitine can quickly be reversed by antiarrhythmic agent lappaconitine. The most interesting fact about these two alkaloids is that they both belong to the subgroup comprised of molecules with lycoctonine skeleton [12]. As it was reported elsewhere [12], there are 4 active regions in aconitine molecule: nitrogen atom of lycoctonine skeleton that acquires a strong positive charge when protonated in a solution, and three functional residues (hydroxyl group at C13, benzoylester group at C14 and acetyl group at C8) playing a crucial role for exhibiting channel opening properties (Fig.1). Interestingly, the absence of any of functional groups mentioned results in blockade of sodium ion channel.

Large numbers of various groups of sodium channel binders have been the targets of extensive multidisciplinary studies including computational approach. This is mainly owing to proven therapeutic value of voltage-gated sodium channel modulators in local anaesthesia, cardiac arrhythmia, pain, epilepsy, stroke and other disorders [8,9]. A literature survey revealed computational and molecular modelling technique have been used primarily for developing QSARs and pharmacophore model generation [14] as 3D x-ray structure of sodium channel is not available yet. These two techniques are considered valuable tools in design of sodium channel modulators and any other drugs of better

efficacy. Moreover, existing parallelism between two or more activities exhibited by $Na^+$ channel binders (for example antiarrhythmic agents posses also local anaesthetic activity) [15] results in highly universal QSAR and pharmacophore models generated.
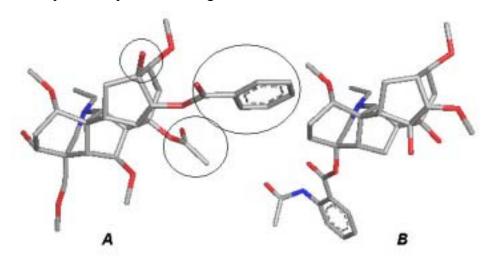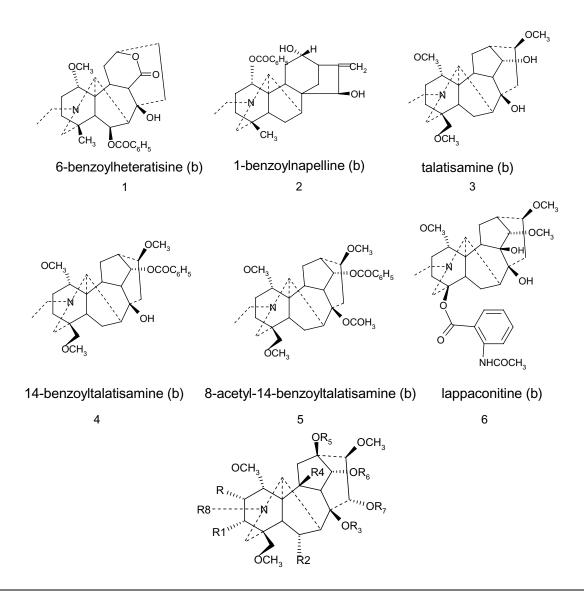


Figure 1.    Aconitine alkaloid molecule (A) with three functional residues responsible for the sodium channel opening activity and its sodium channel antagonist modulator Lappaconitine alkaloid molecule (B)

Though *Delphinium* and *Aconitum* alkaloids have been known for centuries and applied in folk medicine for their analgesic, antirheumatic and neurological indications, they have received little attention of computational chemists. Hence only recently a QSAR analysis of the analgesic and anesthetic properties for 12 *Aconitum* alkaloids has been reported [16,17]. The toxicity/activity data available for these alkaloids and the intriguing sodium channels modulation exhibited (openers and blockers in one homologous series) make them very interesting targets for molecular modelling studies. The present work attempts to shed some light on antagonist $Na^+$ channel modulation of *Delphinium* and *Aconitum* species alkaloids by tracing structure-activity(toxicity) relationship at electronic structure level.

## 2 MATERIALS AND METHODS

### 2.1 Training Compounds

Selection of diterpene alkaloids for quantum-chemical investigations has been performed ensuring an equal number of channel blockers and openers in a series (Fig. 2). Moreover, structures maximally related to aconitine alkaloid (strong activator) but with various combinations of three crucial residues were of the first choice.

6-benzoylheteratisine (b)
1

1-benzoylnapelline (b)
2

talatisamine (b)
3

14-benzoyltalatisamine (b)
4

8-acetyl-14-benzoyltalatisamine (b)
5

lappaconitine (b)
6

| № | Compound name | Functional groups |
|---|---|---|
| 7 | aconine (b) | R1=OH; R2=OCH$_3$; R8=C$_2$H$_5$ |
| 8 | benzoylaconine (b) | R1=OH; R2=OCH$_3$; R6=COC$_6$H$_5$; R8=C$_2$H$_5$ |
| 9 | 3,13,15-threeacetylaconitine (b) | R1=OCOCH$_3$; R2=OCH$_3$; R3=R5=R7=COCH$_3$; R6=COC$_6$H$_5$; R8=C$_2$H$_5$ |
| 10 | aconitine (o) | R1=OH; R2=OCH$_3$; R3=COCH$_3$; R6=COC$_6$H$_5$; R8=C$_2$H$_5$ |
| 11 | aconiphine (o) | R1=R4=OH; R2=OCH$_3$; R3=COCH$_3$; R6=COC$_6$H$_5$; R8=C$_2$H$_5$ |
| 12 | altaconitine (o) | R=R1=OH; R2=OCH$_3$; R3=COCH$_3$; R6=COC$_6$H$_5$; R8=C$_2$H$_5$ |
| 13 | mesaconitine (o) | R1=OH; R2=OCH$_3$; R3=COCH$_3$; R6=COC$_6$H$_5$; R8=CH$_3$ |
| 14 | noraconitine (o) | R1=OH; R2=OCH$_3$; R3=COCH$_3$; R6=COC$_6$H$_5$; R8=H |
| 15 | hyppaconitine (o) | R2=OCH$_3$; R3=COCH$_3$; R6=COC$_6$H$_5$; R8=CH$_3$ |
| 16 | 3-monoacetylaconitine (o) | R1=OCOCH$_3$; R2=OCH$_3$; R3=COCH$_3$; R6=COC$_6$H$_5$; R8=C$_2$H$_5$ |
| 17 | 3,15-diacetylaconitine (o) | R1=OCOCH$_3$; R2=OCH$_3$; R3=R7=COCH$_3$; R6=COC$_6$H$_5$; R8=C$_2$H$_5$ |
| 18 | 3,15- dibenzoylaconitine (o) | R1= COC$_6$H$_5$; R2=OCH$_3$; R3=COCH$_3$; R6=R7=COC$_6$H$_5$; R8=C$_2$H$_5$ |

(b) – sodium channel blocker; (o) – sodium channel opener

Figure 2.    A series of *Aconitum* and *Delphinium* alkaloids studied.

## 2.2 Biological Data

Toxicity data used in this study is taken from the reference [12]. The data suggests alakloids inducing sodium channel activation are more toxic than those alkaloids that block $Na^+$ ion permeation through the channels. All original $LD_{50}$ toxicity data (mg/kg) has been converted to molar $-logLD_{50}$ response variables.

## 2.3 Molecular Modelling

All molecular models were build using the Hyperchem 6.1 software package [18]. The Molecular Mechanics (MM+) force field was applied for preliminary structure optimisation and study of the conformational behaviour of each alkaloid. Molecular mechanics has been shown to produce more realistic geometry values for the majority of organic molecules owing to the fact of being highly parameterised [19]. The next step was a re-optimisation of the MM+ optimised structures in MOPAC 7 package [20] applying PM3 hamiltonian. Quantum mechanical method has been used in order to obtain an accurate charge distribution and the energy of frontier orbitals for each compound in the series.

## 2.4 QSAR and Statistical Software

Preliminary models selection was performed by means of GA-MLRA [21] technique as implemented in the BuildQSAR [22] program. This approach allows selection of the models with the following characteristics: high quadratic correlation coefficient $R^2$, low standard deviation S and the least number of descriptors involved. Next, the NCSS98 [23] professional software package was applied for detailed statistical analysis of the models obtained. Thus, the high Fisher coefficient F, non-collinear descriptors, and the significance level P variable served as additional selection parameters. A final set of QSARs was identified by applying the "leave-one-out" technique with its predicting ability being evaluated and confirmed by cross validation coefficient $Q^2$ based on predictive error sum of squares (SPRESS). Physicochemical descriptors used in this study have been calculated applying the *DRAGON* program [24].

## 3 RESULTS AND DISCUSSION

### 3.1 PM3 Calculations

All 18 compounds included in this study are shown in Fig.2 of which 9 are blockers and other 9 compounds are openers of sodium ion channel. PM3 geometry optimisation followed by detailed investigations of frontier orbitals were carried out in order to reveal whether electronic features of a molecule would reflect the modulation effect nature of the particular alkaloid. Four important molecular orbitals were analysed including highest occupied molecular orbital (HOMO), second

highest molecular orbital (HOMO-1), lowest unoccupied molecular orbital (LUMO) and second lowest unoccupied molecular orbital (LUMO-1). Percentage contributions from each atom to HOMOs and LUMOs are collected in Table 1.

Table 1.    HOMOs and LUMOs main contributors obtained by PM3 method



| Comp | Ground state | | | | | | Protonated Form | | | | |
|------|--------------|---|---|---|---|---|-----------------|---|---|---|---|
| № | HOMO | | | LUMO | | | LUMO | | | HOMO | |
| | Energy, eV | N23S, P(x,y,z) % | C7, C10, C12, C25 % | Energy, eV | O21, C34, O41 % | Benzyl % | Energy, eV | N23S, P(x,y,z) % | C7, C12, C25 % | Energy, eV | Benzyl % |
| 1[*] | -9.044 | 73.84 | 8.32 | -0.304 | – | 96.4 | -3.797 | 35.57 | 49.66 | -12.481 | 98.35 |
| 2[*] | -8.598 | 72.08 | 9.99 | -0.112 | – | 95.29 | -3.376 | 36.0 | 49.05 | -12.482 | 99.54 |
| 3 | -8.735 | 73.51 | 8.99 | 2.472[a] | – | – | -3.548 | 35.63 | 50.33 | -13.164[a] | – |
| 4 | -8.741 | 73.42 | 9.93 | -0.323 | 12.64 | 79.71 | -3.463 | 35.48 | 50.31 | -11.688 | 97.16 |
| 5 | -8.850 | 73.42 | 7.77 | -0.190 | 11.13 | 81.47 | -3.579 | 35.59 | 50.30 | -11.520 | 99.94 |
| 6 | -8.897 | 73.48 | 8.79 | -0.634 | 16.06 | 71.8 | -3.527 | 35.34 | 50.01 | -10.928[b] | 48.47 |
| 7 | -8.951 | 72.96 | 8.63 | 2.290[c] | – | – | -3.216 | 35.50 | 45.90 | -12.920[c] | – |
| 8 | -9.008 | 72.91 | 8.64 | -0.158 | 14.63 | 83.47 | -3.278 | 35.50 | 50.59 | -11.495 | 99.79 |
| 9 | -8.679 | 74.29 | 7.71 | -0.176 | – | 92.71 | -3.051 | 35.56 | 48.53 | -11.669 | 98.43 |
| 10 | -8.940 | 72.94 | 8.55 | -0.333 | 14.32 | 80.2 | -3.205 | 49.24 | 35.51 | -11.658 | 97.73 |
| 11 | -8.944 | 73.09 | 8.28 | -0.436 | 16.53 | 82.48 | -3.186 | 35.71 | 50.48 | -11.705 | 98.89 |
| 12 | -9.043 | 72.9 | 8.8 | -0.387 | 14.53 | 83.3 | -3.480 | 35.51 | 49.59 | -11.739 | 98.08 |
| 13 | -8.934 | 72.56 | 8.23 | -0.334 | 14.3 | 83.68 | -3.265 | 36.31 | 49.39 | -11.655 | 99.19 |
| 14 | -9.156 | 72.4 | 8.42 | -0.298 | 11.67 | 84.73 | -3.312 | 34.65 | 38.68 | -11.701 | 97.08 |
| 15 | -8.759 | 72.52 | 8.05 | -0.287 | 13.8 | 84.14 | -3.465 | 36.26 | 48.62 | -11.683 | 97.99 |
| 16 | -8.646 | 74.36 | 7.64 | 0.142 | – | 91.18 | -3.027 | 35.03 | 49.86 | -11.746 | 98.08 |
| 17 | -8.588 | 74.35 | 7.71 | -0.163 | – | 88.82 | -2.964 | 35.63 | 50.05 | -11.779 | 98.16 |
| 18 | -8.526 | 74.14 | 8.61 | -0.392 | – | 95.4 | -2.880 | 35.71 | 50.04 | -11.739 | 99.51 |

[*]for simplicity reason heteratizine and napelline skeleton have been numbered in the same manner
[a]LUMO: C4 (3.8%), C6 (4.9%), C7 (12.69%), C12 (12.48%), N23 (26.01%), C25 (11.19%)
[a]HOMO: C19 (7.5%), C20 (5.05%)O22 (44.89%), C24 (6.35%),
[b]HOMO: N35 (39.95%), O39(7.58%)

cLUMO: C11 (5.1%), C14 (10.9%), C18 (3.2%), C19 (14.88%), C20 (23.63%), O22 (12.94%), C24 (6.9%)
cHOMO: C14 (2.38%), C18 (2.8%), C19 (11.28%),O30 (19.98%), O29 (2.8%), O32 (20.415)

Molecular orbitals analysis showed two distinct location sites for each HOMO: the HOMOs were mainly represented by contributions of lycoctonine carcass nitrogen atom orbitals, while all the HOMO-1s were comprised of benzoylester's atom orbitals. LUMOs and LUMO-1s were located mostly on benzyl/benzoylester group apart from talatizamine and aconine alkaloids with no such side chain (Table1). No contribution from nitrogen atom orbitals has been detected for these orbitals. The eigenvalues of HOMO and HOMO-1s are found to differ from each other by 0.1 – 1 eV. This fact together with limitations known for semi-empirical methods make one to doubt whether nitrogen atom with the lone electron pair available is a true HOMO or it is more likely a benzyl ring with p-electron system forms this molecular orbital. Interestingly, the HOMO (and HOMO-1) geometries were almost identical for each alkaloid in a set and therefore no difference induced at physicochemical level would be expected. Likewise, after having a close look at LUMOs no substantial features have been identified that would help to distinguish whether particular structure is activator or blocker of $Na^+$ channels. The figure 3 shows LUMOs plotted for benzoylnapelline (strong blocker), benzoylaconine (blocker), aconitine (strong activator) and lappaconitine (strong blocker) that are distributed on benzoylester group irrespectively of its attachment position. Moreover, it clearly demonstrates that three essential functional groups do not participate altogether in this molecular orbital formation: percentage contribution of –OH (in 8 and 10) and $–OCOCH_3$ (in 10) were less than 1. The exception is benzoylester group (about 90-95%) which only contribution is not enough for opening the sodium ion channels.

Toxicity and/or therapeutic action of many medicinal agents strongly depend on solubility of a molecule which subsequently defines its bioavailability. Tertiary nitrogen present in each molecule is a centre with the highest proton affinity and therefore once drug is in water the following reactions occur:

$$H_2O = H^+ + OH^-$$

$$R_3N + H^+ = R_3NH^+$$

The next natural step was to explore re-arranged electronic structure of alkaloids induced by protonation of tertiary nitrogen. The careful examination of molecular orbitals revealed that the orbitals corresponding to nitrogen atom have acquired a lower energy as the result of its protonation. Hence, the HOMO has moved to the zone of inner orbitals, while LUMO has now appeared in the zone of frontier orbitals (Table 1). As can be seen from the table 1, protonated nitrogen and its closest neighbouring carbon atoms have now comprised LUMO, while HOMO is represented by benzyl group

6

only. The small changes in locations of molecular orbitals have been observed. Thus LUMO has slightly shifted towards C7, C12 and C25 atoms with nitrogen atom contribution being decreased twice. The HOMOs have been located exclusively on benzyl ring for each alkaloid with no ester group contribution. Again, close values of LUMO and LUMO-1 ($\leq$ 1.5 eV) have been observed for protonated forms of alkaloids.
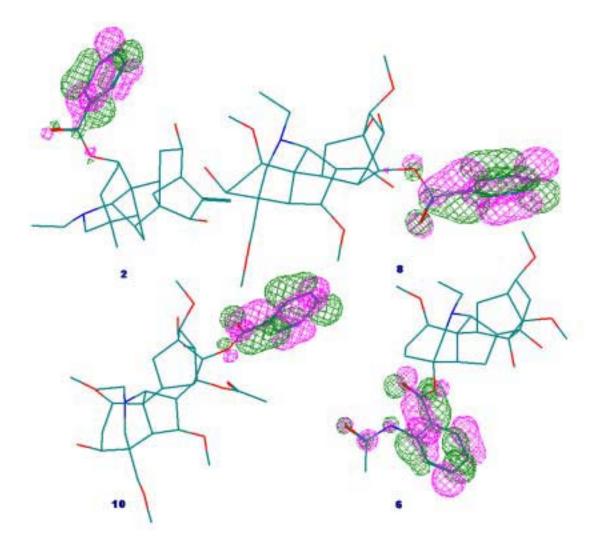


Figure 3.    LUMO isosurfaces of benzoylnapelline 2, benzoylaconine 8, aconitine 10 and lappaconitine 6 (positive – green; negative – violet)

The latter observations have shown, that antagonist modulating action of *Aconitum* and *Delphinium* diterpene alkaloids are likely to be regulated by allosteric interactions and not by frontier orbitals.

## 3.2 QSAR Analysis

The next approach to be applied was QSAR analysis. Aiming to identify which of physicochemical descriptors (molar refractivity MR, molecular weight, MW, lypophilicity MlogP etc.) or quantum-chemical characteristics (energy of HOMO, Energy of LUMO, HOMO and LUMO energy gap calculated for both ground and protonated states) correlates best with toxicity data we built several QSAR models. The statistical significance of each model is evaluated by the correlation coefficient **r**, standard error **s**, adjusted r-squared $\mathbf{r^2_{adj}}$, **F**-test value, significance level of the model **P**, leave-one-out cross-validation coefficient $\mathbf{Q^2}$ and predictive error sum of squares **SPRESS**. The descriptors [25] used in this study are collected in Tables 2 and 3.

Table 2.        Physicochemical descriptors applied in this study

| Alkaloid | $LD_{50}$ mg/kg[*] | $\log LD_{50}^{-1}$ (molar) | MR | TPSA | MlogP | MW | nHDon | nHAcc |
|---|---|---|---|---|---|---|---|---|
| 6-benzoylheteratizine | 5.0 | 5.0 | 127.993 | 65.07 | 3.847 | 495.67 | 3 | 7 |
| 1-benzoylnapelline | 30 | 4.19 | 126.113 | 29.54 | 4.566 | 463.67 | 2 | 5 |
| Talatisamine | 110.0 | 3.58 | 110.138 | 30.93 | 2.232 | 421.64 | 4 | 6 |
| 14-benzoyltalatisamine | 25.0 | 4.32 | 139.463 | 57.23 | 3.504 | 525.75 | 3 | 7 |
| 8-acetyl-14-benzoyl-talatisamine | 15.0 | 4.58 | 148.614 | 83.53 | 3.855 | 567.79 | 0 | 8 |
| Lappaconitine | 5.9 | 5.0 | 148.91 | 74.3 | 2.061 | 584.78 | 7 | 10 |
| Aconine | 200 | 3.4 | 119.932 | 40.16 | -0.537 | 499.67 | 9 | 10 |
| Benzoylaconine | 16 | 4.58 | 149.256 | 66.46 | 0.75 | 603.78 | 8 | 11 |
| 3,13,15-threeacetylaconitine | 150 | 3.71 | 185.862 | 171.66 | 2.263 | 771.94 | 0 | 15 |
| Aconitine | 0.125 | 6.71 | 158.408 | 92.76 | 1.127 | 645.82 | 5 | 12 |
| Aconiphine | 0.22 | 6.48 | 159.532 | 92.76 | 0.416 | 661.82 | 8 | 13 |
| Altaconitine | 2.2 | 5.48 | 159.505 | 92.76 | 0.416 | 661.82 | 6 | 13 |
| Mesaconitine | 0.085 | 6.87 | 153.66 | 92.76 | 0.944 | 631.79 | 5 | 12 |
| Noraconitine | 0.15 | 6.61 | 148.763 | 89.52 | 0.759 | 617.76 | 6 | 12 |
| Hyppaconitine | 0.16 | 6.58 | 152.187 | 92.76 | 1.661 | 615.79 | 4 | 11 |
| 3-monoacetylaconitine | 0.27 | 6.4 | 167.559 | 119.06 | 1.506 | 687.86 | 4 | 13 |
| 3,15-diacetylaconitine | 3.5 | 5.31 | 176.711 | 145.36 | 1.885 | 729.9 | 3 | 14 |
| 3,15-dibenzoylaconitine | 13.2 | 4.81 | 217.056 | 145.36 | 3.64 | 854.04 | 3 | 14 |

[*] $LD_{50}$ values have been taken from reference [12]

MR – Ghose-Grippen Molar Refractivity, TPSA – Topological Polar Surface Area, MlogP – Moriguchi octanol-water partition coefficient (DRAGON code),MW – Molecular Weight, nHDon – number of donor atoms for H-bonds (with N and O atoms), nHAcc – number of acceptor atoms (N, O, F)

As a result, no equation with good statistical quality was obtained. The MW values were plotted against toxicity data to obtain a graphical representation of relationship if any exist. The plot (Fig. 4) suggested there are two independent linear relationships: the red points correspond to arrhythmogenic alkaloids that cause persistent activation of sodium channel, whereas the blue ones correspond to

antiarrhythmic alkaloids that block sodium channels. Two possible outliners have been also detected on this graph. These are altaconitine for the openers' set and 3,13,15-threeacetylaconitine for the blockers' set.

Table 3.        Quantum-chemical descriptors applied in this study

| Alkaloid | HOMO | LUMO | GAP | HOMO Proton | LUMO Proton | GAP Proton |
|---|---|---|---|---|---|---|
| 6-benzoylheteratizine | -9.044 | -0.304 | 8.74 | -12.481 | -3.797 | 8.684 |
| 1-benzoylnapelline | -8.598 | -0.112 | 8.486 | -12.482 | -3.376 | 9.106 |
| Talatisamine | -8.735 | 2.472 | 11.207 | -13.164 | -3.548 | 9.616 |
| 14-benzoyltalatisamine | -8.741 | -0.323 | 8.418 | -11.686 | -3.463 | 8.223 |
| 8-acetyl-14-benzoyl-talatisamine | -8.85 | -0.19 | 8.66 | -11.52 | -3.579 | 7.941 |
| Lappaconitine | -8.897 | -0.634 | 8.263 | -10.928 | -3.527 | 7.401 |
| Aconine | -8.951 | 2.29 | 11.241 | -12.92 | -3.216 | 9.704 |
| Benzoylaconine | -9.008 | -0.158 | 8.85 | -11.495 | -3.278 | 8.217 |
| 3,13,15-threeacetylaconitine | -8.679 | -0.176 | 8.503 | -11.669 | -3.051 | 8.618 |
| Aconitine | -8.94 | -0.333 | 8.607 | -11.658 | -3.205 | 8.453 |
| Aconiphine | -8.944 | -0.436 | 8.508 | -11.705 | -3.186 | 8.519 |
| Altaconitine | -9.043 | -0.387 | 8.656 | -11.739 | -3.480 | 8.259 |
| Mesaconitine | -8.934 | -0.334 | 8.6 | -11.690 | -3.261 | 8.429 |
| Noraconitine | -9.156 | -0.298 | 8.858 | -11.701 | -3.312 | 8.389 |
| Hyppaconitine | -8.759 | -0.287 | 8.472 | -11.683 | -3.465 | 8.218 |
| 3-monoacetylaconitine | -8.646 | -0.142 | 8.504 | -11.746 | -3.027 | 8.719 |
| 3,15-diacetylaconitine | -8.588 | -0.163 | 8.425 | -11.779 | -2.964 | 8.815 |
| 3,15-dibenzoylaconitine | -8.526 | -0.392 | 8.134 | -11.739 | -2.880 | 8.859 |

HOMO – Energy of Highest Occupied Molecular Orbital, LUMO – Energy of Lowest Unoccupied Molecular Orbital, GAP – HOMO-LUMO energy gap, HOMO_Proton, LUMO_Proton, GAP_Proton – Energy of HOMO, LUMO and HOMO-LUMO energy gap for the protonated forms
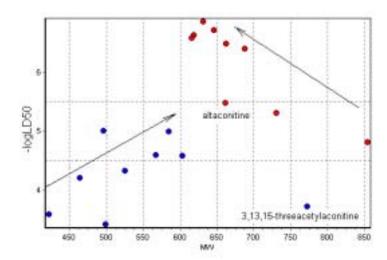


Figure 4.        2D plot Toxicity versus descriptor MW

### 3.2.1 Na$^+$ channel activator alkaloids

As it was found earlier, the affinities of these alkaloids to sodium channels correlate with their effective doses (ED$_{50}$) determined for acute toxicity [9]. The values of therapeutic index (LD$_{50}$/ED$_{50}$) are in the range from 1 to 6. This suggests the models obtained for structure-toxicity relationship might also be considered as the true ones for structure-channel affinity relationship and be applied for rational channel openers design. Several runs of GA-MLRA technique have selected physicochemical descriptors (MW, MR, TPSA, MlogP) as the ones correlating best with the LD$_{50}$ data among the rest of descriptors. However, despite of high correlation coefficient values, the overall statistical fit of the equations was not acceptable due to low values of cross-validation coefficients. 2D plotting of these descriptors against toxicity has indicated altaconitine as the most probable deviant (Fig. 4). Examination of altaconitine structure with its toxicity data extrapolated from the set of compounds LD$_{50}$ has shown the former one likely being underestimated experimentally. Thus the structure of altaconitine is very similar to aconitine alkaloid with only difference in functional residue R (Fig. 2). Indeed the exclusion of this compound from the data set results in significant improvement of statistical quality of new equations obtained:

$$\text{Log}(LD_{50}^{-1}) = -0.00872(\pm0.00310)\ \textbf{MW} +12.15872(\pm2.125515) \tag{1}$$
$$n=8;\ r=0.94;\ r^2_{adj}=0.88\ s=0.28;\ F=44.171;\ P=0.00056;\ Q^2=0.76;\ \text{SPRESS}=0.39$$

$$\text{Log}(LD_{50}^{-1}) = -0.02841(\pm0.01043)\ \textbf{TPSA} +9.31167(\pm1.159815) \tag{2}$$
$$n=8;\ r=0.94;\ r^2_{adj}=0.85\ s=0.29;\ F=41.47;\ P=0.000664;\ Q^2=0.75;\ \text{SPRESS}=0.40$$

$$\text{Log}(LD_{50}^{-1}) = -0.63873(\pm0.37324)\ \textbf{MlogP} +7.17439(\pm0.656371) \tag{3}$$
$$n=8;\ r=0.86;\ r^2_{adj}=0.69\ s=0.42;\ F=16.38;\ P=0.006748;\ Q^2=0.60;\ \text{SPRESS}=0.51$$

$$\text{Log}(LD_{50}^{-1}) = -0.03081(\pm0.01247)\ \textbf{MR} +11.35844(\pm2.094641) \tag{4}$$
$$n=8;\ r=0.92;\ r^2_{adj}=0.83;\ s=0.31;\ F=34.17;\ P=0.001106;\ Q^2=0.55;\ \text{SPRESS}=0.54$$

Owing to small number of compounds available we aimed to obtain rather qualitative picture by identifying properties that most related to toxicity. All four equations are equally good fitted. According to the models generated increase of molecular mass MW, heteroatom associated surface area TPSA and hydrophobicity MlogP results in compounds exhibiting less toxicity. Four selected descriptors appeared to be highly collinear with each other and therefore mono-descriptor containing models only are presented in this work. High collinearity of molecular weight with hydrophobicity indicates the series of compounds is homologous and there is a chance that true relationship between

activity/toxicity and physicochemical properties may be lost or hidden [26]. However, equation 2 suggests that heteroatoms present in a molecule also alter toxicity. Assuming Eq.2 and Eq.3 indicate increase of polar and bulky parts of a molecule respectively then it becomes clear that molecular size is a parameter most important mechanistically. The equation 4 also supports this idea as MR descriptor accounts for two main characteristics of a molecule – its both polarizability and molecular volume. The most relevant descriptor controlling the endpoint of interest should be selected while developing mechanistically based QSAR models [27]. For the studied set of alkaloids descriptors related to molecular size (MW, MR) are identified as important properties to model the ability of alkaloid to reach the site of action (site 2 on voltage-gated sodium channel). The obtained models suggest that compact structure of a toxicant and smaller molecular weight improves the chances of alkaloid to reach the target site.

### 3.2.2 Na$^+$ channel blocker alkaloids

In contrast to the openers of the ion channel, toxicity of blockers has shown a good correlation with quantum-chemical descriptors. In particular, energy of LUMO and the HOMO-LUMO energy gap turned to be descriptors most relevant to toxicity exerted by the antiarrhythmic alkaloids. However, 3,13,15-threeacetylaconitine has been omitted from the final equations for obtaining models with better statistical fits. Again, the compound differs from the aconitine alkaloid by having two additional –OCOCH$_3$ at R5 and R7, and at the R1 instead of –OH key group (Fig. 2).

$$\text{Log}(LD_{50}^{-1}) = -0.43087(\pm 0.19680) \text{ LUMO} +4.49503(\pm 0.241308) \tag{5}$$
$$n=8; \ r=0.90; \ r^2_{adj}=0.79; \ s=0.27; \ F=26.81; \ P=0.002059; \ Q^2=0.70; \ \text{SPRESS}=0.35$$

$$\text{Log}(LD_{50}^{-1}) = -0.41207(\pm 0.23389) \text{ GAP} +8.13592(\pm 2.176595) \tag{6}$$
$$n=8; \ r=0.86; \ r^2_{adj}=0.70; \ s=0.33; \ F=17.36; \ P=0.005901; \ Q^2=0.61; \ \text{SPRESS}=0.40$$

As it was mentioned before, the receptor site for these alkaloids might be located very close to or even to be overlapped with the site for channel openers. It is very natural that other descriptors might be responsible for demonstration of such properties or even the ones identified for the openers but having an opposite sign. Extensive QSAR (including 3D-QSAR) studies on various groups of sodium channel blockers have been reported in a number of papers and the energy of LUMO was identified as one of the most influential descriptors [28]. LUMO describes electrophilic reactivity and the models containing it are straightforward to explain. Our model shows that lower LUMO energy favoring electron acceptor properties is associated with high toxicity. The same trend is observed for the

HOMO-LUMO energy gap. The equation 6 suggests that alkaloids with larger HOMO-LUMO energy gap (i.e more stable molecules) are less toxic accordingly.

# 4 CONCLUSIONS

Antagonist modulation of voltage-gated sodium channels exhibited by *Aconitum* and *Delphinium* plant species alkaloids have been investigated by means of two computational approaches: analysis of frontier MOs generated by semiempirical PM3 method and a QSAR study. An examination of HOMO (HOMO-1) and LUMO (LUMO-1) for both ground and protonated forms of each molecule has been carried out in order to estimate contributions of three crucial residues responsible for channel opening activity into these orbitals. It was shown that HOMO (ground state) and LUMO (protonated state) were mainly comprised of nitrogen atom orbitals, while LUMO and HOMO for ground and protonated states respectively were located on benzyl/benzoyl side chain for majority of alkaloids. The contribution values of –OH and –OCOCH$_3$ groups into frontier orbitals were found to be negligibly low (about 1% in total). The results obtained from this piece of research have confirmed the experimental findings suggesting neurotoxins acting at type 2 receptor site are allosteric modulators of voltage-dependent sodium channel function. Thus it was concluded that activation/blockade of the channel caused by each particular alkaloid are not regulated by frontier orbitals but rather depends on whether specific functional groups are present in a molecule structure.

QSAR models generated separately for each set of alkaloids (blockers and activators of sodium channel) have also indicated their difference in modulation activity. QSARs built for the channel activators showed the importance of the molecular size descriptors confirming that small molecules exert stronger toxicity due to higher chances of reaching the receptor site. For the set of blockers, the energy of LUMO and HOMO-LUMO energy gap have been selected as the toxicity-defining descriptors. Thus strong electrophilicity (LUMO) and lower stability of the molecule (GAP) are associated with highly toxic alkaloids.

## Supplementary Material

Table 4.    Experimental, Calculated and Residual values of toxicity data for the QSAR models generated

| Compound | Exp $\log LD_{50}^{-1}$ | Equation 1 | | Equation 2 | | Equation 3 | | Equation 4 | |
|---|---|---|---|---|---|---|---|---|---|
| | | Calc | Res | Calc | Res | Calc | Res | Calc | Res |
| Aconitine | 6.71 | 6.525 | 0.185 | 6.677 | 0.033 | 6.455 | 0.256 | 6.478 | 0.232 |
| Aconiphine | 6.48 | 6.385 | 0.095 | 6.677 | -0.197 | 6.909 | -0.429 | 6.443 | 0.037 |
| Mesaconitine | 6.87 | 6.647 | 0.223 | 6.677 | 0.193 | 6.571 | 0.299 | 6.624 | 0.246 |
| Noraconitine | 6.61 | 6.769 | -0.159 | 6.769 | -0.159 | 6.690 | -0.080 | 6.775 | -0.165 |
| Hyppaconitine | 6.58 | 6.787 | -0.207 | 6.677 | -0.097 | 6.114 | 0.467 | 6.670 | -0.090 |
| 3-Mono-acetylaconitine | 6.4 | 6.158 | 0.242 | 5.930 | 0.470 | 6.213 | 0.188 | 6.196 | 0.204 |
| 3,15-Diacetyl-aconitine | 5.31 | 5.791 | -0.481 | 5.183 | 0.128 | 5.970 | -0.660 | 5.914 | -0.604 |
| 3,15-Dibenzoyl-aconitine | 4.81 | 4.708 | 0.102 | 5.183 | -0.373 | 4.849 | -0.039 | 4.671 | 0.139 |

| Compound | Exp $\log LD_{50}^{-1}$ | Equation 5 | | Equation 6 | |
|---|---|---|---|---|---|
| | | Calc | Res | Calc | Res |
| 6-Benzoylheteratizine | 5.0 | 4.626 | 0.374 | 4.535 | 0.466 |
| 1-Benzoylnapelline | 4.19 | 4.543 | -0.353 | 4.639 | -0.449 |
| Talatisamine | 3.58 | 3.430 | 0.150 | 3.518 | 0.062 |
| 14-Benzoyltalatisamine | 4.32 | 4.634 | -0.314 | 4.667 | -0.347 |
| 8-Acetyl-14-benzoyl-talatisamine | 4.58 | 4.577 | 0.003 | 4.567 | 0.013 |
| Lappaconitine | 5.0 | 4.768 | 0.232 | 4.731 | 0.269 |
| Aconine | 3.4 | 3.508 | -0.108 | 3.504 | -0.104 |
| Benzoylaconine | 4.58 | 4.563 | 0.0169 | 4.489 | 0.091 |

Table 5.    Correlation matrix for physicochemical and quantum-chemical descriptors used in this study.

| | MR | PSA | MlogP | MW | nHDon | nHAcc | HOMO Proton | LUMO Proton | GAP Proton | HOMO | LUMO | GAP |
|---|---|---|---|---|---|---|---|---|---|---|---|---|
| MR | 1 | .83 | .001 | .964 | .058 | .661 | .34 | .523 | .066 | .152 | .306 | .393 |
| PSA | | 1 | .002 | .879 | .118 | .737 | .263 | .452 | .044 | .113 | .224 | .288 |
| MlogP | | | 1 | .021 | .616 | .273 | .003 | .071 | .004 | .279 | .053 | .114 |
| MW | | | | 1 | .018 | .825 | .327 | .578 | .053 | .085 | .262 | .32 |
| nHDon | | | | | 1 | .024 | 0 | .001 | .000 | .336 | .043 | .106 |
| nHAcc | | | | | | 1 | .25 | .55 | .028 | .001 | .122 | .123 |
| HOMO Proton | | | | | | | 1 | .034 | .815 | .007 | .675 | .63 |
| LUMO Proton | | | | | | | | 1 | .066 | .227 | .007 | .032 |
| GAP Proton | | | | | | | | | 1 | .086 | .597 | .493 |
| HOMO | | | | | | | | | | 1 | .002 | .027 |
| LUMO | | | | | | | | | | | 1 | .958 |
| GAP | | | | | | | | | | | | 1 |

# 5 REFERENCES

[1] J. J. Clare, S. N. Tate, M. Nobbs and M. Romanos, Voltage-Gated Sodium Channels as Therapeutic Targets, *DDT*, **2000**, 5, 506-520

[2] W. A. Catterall, A 3D View of Sodium Channels, *Nature*, **2001**, 409, 988-991

[3] M. D. Baker and J. N. Wood, Involvement of Na$^+$ Channels in Pain Pathways, *TiPS*, **2001**, 22, 27-31

[4] C. P. Taylor and B. S. Meldrum, Na$^+$ Channels as Targets for Neuroprotective Drugs, *TiPS*, **1995**, 16, 309-916

[5] S. Cestele, W. A. Catterall, Molecular Mechanisms of Neurotoxin Action on Voltage-Gated Sodium Channels, *Biochimie*, **2000**, 82, 883-892

[6] S.-Y. Wang, G. K. Wang, Voltage-gated Sodium Channels as Primary Targets of Diverse Lipid-soluble Neurotoxins, *Cell. Sign.*, **2003**, 15, 151-159

[7] T. Anger, D. J. Madge, M. Mulla, and D. Riddal, Medicinal Chemistry of Neuronal Voltage-Gated Sodium Chanel Blockers, *J. Med. Chem.*, **2001**, 44, 115-137

[8] A Ameri., The Effects of *Aconitum* Alkaloids on the Central Nervous System, *Prog. Neurobiol.* **1998**, *56*, 211

[9] J. Friese, J. Gleitz, U. T. Guster, J. F. Heubach, T. Matthiesen, B. Wilffert, N. Selve, *Aconitum* sp. Alkaloids: the Modulation of Voltage-Dependent Na$^+$ Channels, Toxicity and Antinociceptive Properties, *Eur. J. Pharmacol.*, **1997**, 337, 165-174

[10] S. N. Wright, Irreversable Block of Human Heart (hH1) Sodium Channels by the Plant Alkaloid Lappaconitine, *Mol. Pharmacol.*, **2001**, 59, 183-192

[11] J. F. Heubach,; A. Schule, Cardiac Effects of Lappaconitine and N-deacetyllappaconitine, Two Diterpenoid Alkaloids from Plants of the *Aconitum* and *Delphinium*, *Planta Med.* **1998**, *64*, 22

[12] F. N. Dzhakhangirov, M. N. Sultankhodzhaev,. B. Tashkhodzhaev, B. T. Salimov, *Chem. Nat. Comp.* **1997**, *33*, 190

[13] A. Ameri, T. Simmet, Interaction of the Structurally Related *Aconitum* Alkaloids, Aconitine and 6-benzoylheteratisine, in the Rat Hippocampus, *Eur. J. Pharmacol.*, **1999**, 386, 187-194

[14] Y. Li and W.E. Harte, A Review of Molecular Modeling Approaches to Pharmacophore Models and Structure-Activity Relationships of Ion Channel Modulators in CNS, *Curr. Pharm. Des.*, **2002**, 8, 99-110

[15] S. P. Gupta, Quantative Structure-Activity Relationships of Antiarrhythmic Drugs, Curr. *Pharm. Des.,* **1998**, 4, 455-468

[16] A.M. Bello-Ramirez, J. Buendia-Orozco, A.A. Nava-Ocampo, A QSAR Analysis to Explain the Analgesic Properties of *Aconitum* alkaloids, *Fundam. Clin. Pharmacol.* **2003**, *17*, 575-580

[17] A.M. Bello-Ramirez, A.A. Nava-Ocampo, The Local Anesthetic Activity of *Aconitum* Alkaloids Can Be Explained by Their Structural Properties, A QSAR Analysis, *Fundam. Clin. Pharmacol.* **2004**, *18*, 157-161

[18] HyperChem 6.01 (HyperCube, Inc), **2000**

[19] D.Young, *Computational Chemistry: A Practical Guide for Applying Techniques to Real World Problems*; John-Wiley & Sons: New York (USA), **2001**

[20] Stewart, J. J. P., J. Comput.-Aid. Mol. Des., 1990, 4, 1

[21] J.Devillers, *Genetic Algorithms in Molecular Modeling*; Academic Press Ltd.: London, (U.K.), **1996**

[22] D.B.de Oliveira, A.C.Gaudio, *Quant. Struct.-Act. Relat.* **2000**, *19*, 599

[23] Statistical analysis software NCSS98, trial version, **1998**

[24] R. Todeschini, V. Consonni, DRAGON software for the Calculation of Molecular Descriptors, Web version 3.0 for Windows

[25] R. Todeschini, V. Consonni, *Handbook of Molecular Descriptors*; Mannhold R., Kubinyi H., Timmerman H., Eds.; Wiley-VCH: Weinheim, New York, **2000**

[26] M.T.D. Cronin, T. W. Schultz, Pitfalls in QSAR, *J. Mol. Struct. (Theochem)* **2003**, *622*, 39-51

[27] T. W. Schultz, M. T. D. Cronin, J. D. Walker, A. O. Aptula, Quantative Structure- Activity Relationships (QSARs) in Toxicology: A Historical Perspective, *J. Mol. Struct. (Theochem)* **2003**, *622*, 1-22

[28] M. L. Brown, C. C. Zha, C. C. V. Dyke, G. B. Brown, and W. J. Brouillette, Comparative Molecular Field Analysis of Hydantoin Binding to the Neuronal Voltage-Dependent Sodium Channel, *J. Med. Chem.*, **1999**, 42, 1537-1545